

Screening of novel immunogenic cell death inducers within the NCI Mechanistic Diversity Set

Abdul Qader Sukkurwala^{1,2,3}, Sandy Adjemian^{1,2,3}, Laura Senovilla^{1,2,3,4}, Michael Michaud^{1,2,3}, Sabrina Spaggiari^{1,2,5}, Erika Vacchelli^{1,2,3}, Elisa Elena Baracco^{1,2,3}, Lorenzo Galluzzi^{1,2,3,6}, Laurence Zitvogel^{3,4,7,8}, Oliver Kepp^{1,2,5,*}, and Guido Kroemer^{1,2,5,6,9,*}

¹Equipe 11 labellisée par la Ligue Nationale contre le cancer; Centre de Recherche des Cordeliers; Paris, France; ²INSERM U1138; Paris, France; ³Gustave Roussy Comprehensive Cancer Center; Villejuif, France; ⁴INSERM, U1015; Villejuif, France; ⁵Metabolomics and Cell Biology Platforms; Gustave Roussy Comprehensive Cancer Center; Villejuif, France; ⁶Université Paris Descartes/Paris 5; Sorbonne Paris Cité; Paris, France; ⁷Université de Paris Saclay; Faculté de Médecine; Le Kremlin Bicêtre, France; ⁸Center of Clinical Investigations in Biotherapies of Cancer (CICBT) 507; Villejuif, France; ⁹Pôle de Biologie; Hôpital Européen Georges Pompidou; AP-HP; Paris, France

Keywords: apoptosis, autophagy, C57BL/6 mice, dendritic cells, HTS, mitoxantrone

Abbreviations: CRT, calreticulin; ER, endoplasmic reticulum; FDA, Food and Drug Administration; FBS, fetal bovine serum; GFP, green fluorescent protein; HMGB1, high mobility group box 1; ICD, immunogenic cell death; NCI, National Cancer Institute; PI, propidium iodide

Immunogenic cell death (ICD) inducers can be defined as agents that exert cytotoxic effects while stimulating an immune response against dead cell-associated antigens. When initiated by anthracyclines, ICD is accompanied by stereotyped molecular changes, including the pre-apoptotic exposure of calreticulin (CRT) on the cell surface, the lysosomal secretion of ATP during the blebbing phase of apoptosis, and the release of high mobility group box 1 (HMGB1) from dead cells. By means of genetically engineered human osteosarcoma U2OS cells, we screened the 879 anticancer compounds of the National Cancer Institute (NCI) Mechanistic Diversity Set for their ability to promote all these hallmarks of ICD in vitro. In line with previous findings from our group, several cardiac glycosides exhibit a robust propensity to elicit the major manifestations of ICD in cultured neoplastic cells. This screen pointed to septacidin, an antibiotic produced by *Streptomyces fibriatus*, as a novel putative inducer of ICD. In low-throughput validation experiments, septacidin promoted CRT exposure, ATP secretion and HMGB1 release from both U2OS cells and murine fibrosarcoma MCA205 cells. Moreover, septacidin-killed MCA205 cells protected immunocompetent mice against a re-challenge with live cancer cells of the same type. Finally, the antineoplastic effects of septacidin on established murine tumors were entirely dependent on T lymphocytes. Altogether, these results underscore the suitability of the high-throughput screening system described here for the identification of novel ICD inducers.

Introduction

Traditionally, anticancer agents are developed according to a preclinical “pipeline” that involves several steps. First, chemicals are probed for their cytostatic and cytotoxic activity on cultured human cancer cells. Second, selected compounds are evaluated for their anticancer effects on human neoplasms developing in severely immunodeficient mice. Alongside, the same compounds are generally subjected to strict toxicological evaluations in various animal species.¹⁻³ This procedure is widely applied and the National Cancer Institute (NCI) has been launching or supporting initiatives to test tens of thousands of putative anticancer agents on a panel of 60 human cancer cell lines representing different types of malignancy. As a result of these efforts, a relative small collection of compounds (879 among the 37 836 initially available) has been selected to represent a broad range of growth inhibition patterns, yielding the so-called Mechanistic Diversity Set. This drug library is freely available to

investigators worldwide (source http://dtp.nci.nih.gov/branches/dscb/mechanistic_explanation.html).

Although for a long time antineoplastic agents were assumed to operate mostly via cancer cell-autonomous mechanisms, i.e., by directly inhibiting the proliferation or triggering the demise of malignant cells, accumulating evidence indicates that multiple chemotherapeutics that have been successfully employed in the clinics for decades also elicit novel (or reactivate silent) anticancer immune responses.³⁻⁷ Thus, anthracyclines loose their therapeutic activity in mice bearing transplantable as well as chemically or transgene-induced tumors if the host immune system is compromised by pharmacological or genetic interventions, such as the injection of CD8⁺ T cell-depleting antibody or the knockout of recombination activating gene 2 (*Rag2*), respectively. Conversely, these conventional antineoplastic agents exert optimal effects when the immune system is intact, both in rodent tumor models and in cancer patients, a setting that allows for the (re)activation of anticancer immunosurveillance.⁸⁻¹⁶

*Correspondence to: Guido Kroemer; Email: kroemer@orange.fr; Oliver Kepp; Email: oliver.kepp@gustaveroussy.fr

Submitted: 02/12/2014; Accepted: 03/08/2014; Published Online: 04/16/2014

Citation: Sukkurwala AQ, Adjemian S, Senovilla L, Michaud M, Spaggiari S, Vacchelli E, Elena Baracco E, Galluzzi L, Zitvogel L, Kepp O, et al. Screening of novel immunogenic cell death inducers within the NCI Mechanistic Diversity Set. *Oncoimmunology* 2014; 3:e28473; <http://dx.doi.org/10.4161/onci.28473>

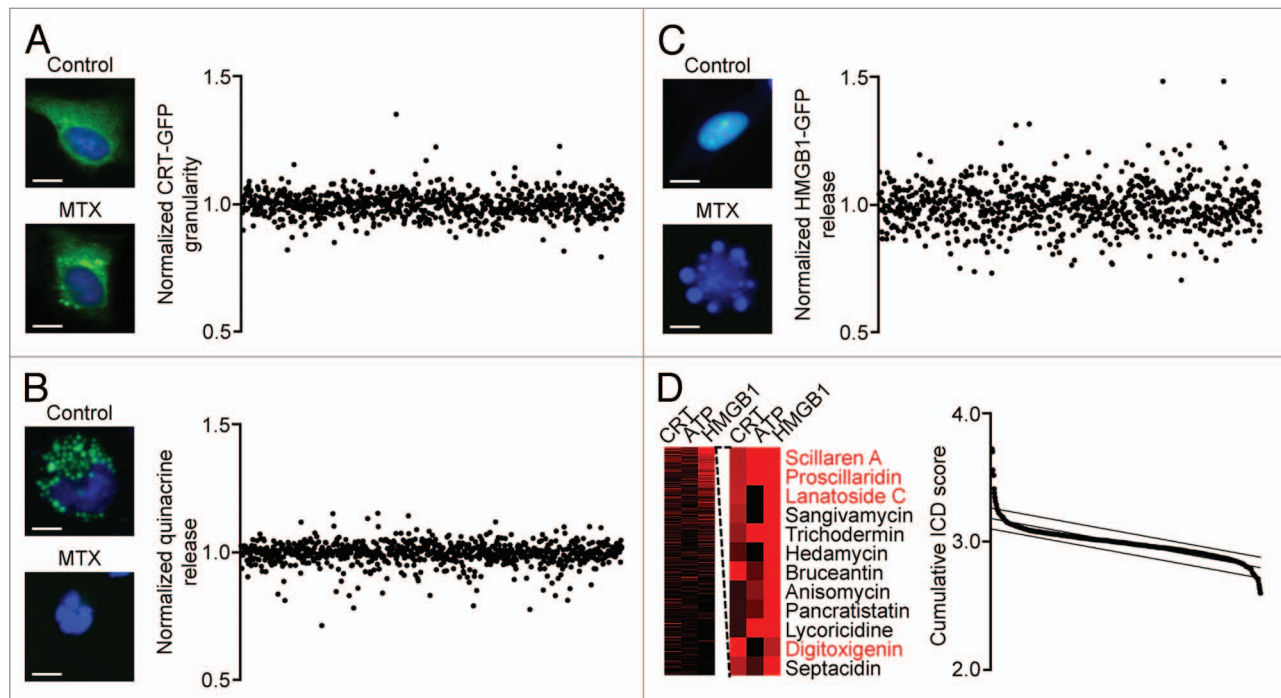


Figure 1. A fluorescence microscopy-based screening platform for the identification of immunogenic cell death inducers. **A–C.** Wild-type (WT) human osteosarcoma U2OS cells or U2OS cells stably co-expressing H2B-RFP and CRT-GFP or HMGB1-GFP were treated with compounds from the NCI Mechanistic Diversity Set (final concentration = 1 μ M) for 4, 24, or 48 h, followed by the assessment of CRT-GFP redistribution (**A**), loss of quinacrine-dependent fluorescence (**B**) and HMGB1 release (**C**), respectively, by automated fluorescence microscopy. Representative images (scale bars = 10 μ m) and quantitative data are depicted. Each point represents the average of duplicate assessments obtained for each drug, upon intra-plate normalization. (**D**) Quantitative data as obtained in A–C are depicted as a heat map. The scores associated with each immunogenic cell death (ICD)-related phenomenon were summed up to assign to each compound of the NCI Mechanistic Diversity Set a cumulative ICD score. Compounds belonging to the top 1% percentile of the resulting rank are shown (cardiac glycosides in red). See also **Table S1**.

One of the mechanisms through which anthracyclines exert immunostimulatory effects relies on immunogenic cell death (ICD), a non-conventional type of apoptosis that is associated with the activation of an adaptive immune response against dead cell-associated antigens.^{14–16} Thus, upon subcutaneous delivery to immunocompetent mice in the absence of any adjuvant, murine cancer cells undergoing ICD are able to elicit an immune response that protects the animals against a subsequent challenge with living cells of the same type. Importantly, only a few stimuli have been shown to induce bona fide ICD so far, including various anthracyclines (e.g., doxorubicin, epirubicin, mitoxantrone), cyclophosphamide, oxaliplatin, ionizing irradiation, and hypericin-based photodynamic therapy.^{17–21}

Using anthracyclines as model ICD inducers, we have been characterizing the molecular mechanisms that differentiate immunogenic from non-immunogenic instances of cell death. So far, we have identified 3 major mechanisms that are required (though perhaps not sufficient) for dying cells to stimulate adaptive immunity: (1) the early, pre-apoptotic exposure of calreticulin (CRT) on the cell surface, which originates from the activation of an endoplasmic reticulum (ER) stress response;^{19,22–24} (2) the autophagy-dependent, lysosomal secretion of ATP via caspase-activated pannexin 1 channels;^{12,25–28} and (3) the release into the extracellular space of the nuclear protein high mobility group box 1 (HMGB1), as this can occur during secondary necrosis.^{29–32}

By binding to specific pattern recognition receptors expressed by myeloid cells, including (but perhaps not limited to) CD91, purinergic receptor P2X, ligand-gated ion channel, 7 (P2RX7), purinergic receptor P2Y, G-protein coupled, 2 (P2YR2), and Toll-like receptor 4 (TLR4), CRT, ATP, and HMGB1 attract dendritic cell precursors to the proximity of dying cancer cells and stimulate them to take up dead cell-associated antigens, mature, and ignite cytotoxic T-lymphocyte responses.^{9,12,33}

Based on this knowledge, we developed an automated screening platform enabling the identification of compounds that induce CRT exposure, ATP secretion, and HMGB1 release (in vitro) within large chemical libraries. We first tested this platform on the ensemble of anticancer agents that are currently approved by the US Food and Drug Administration (FDA), unveiling the unsuspected ability of several cardiac glycosides (including digoxin and digitoxin) to render cell death immunogenic.^{34–36} Thus, digoxin and digitoxin turned out to convert the immunologically silent demise of murine cancer cells exposed to cisplatin or mitomycin C into bona fide ICD, as determined in vaccination experiments. Moreover, cardiac glycosides improved the efficacy of non-immunogenic chemotherapeutics against tumors established in immunocompetent, but not immunodeficient, mice. Finally, we found that a cohort of carcinoma patients receiving cardiac glycosides along with non-immunogenic chemotherapy (owing

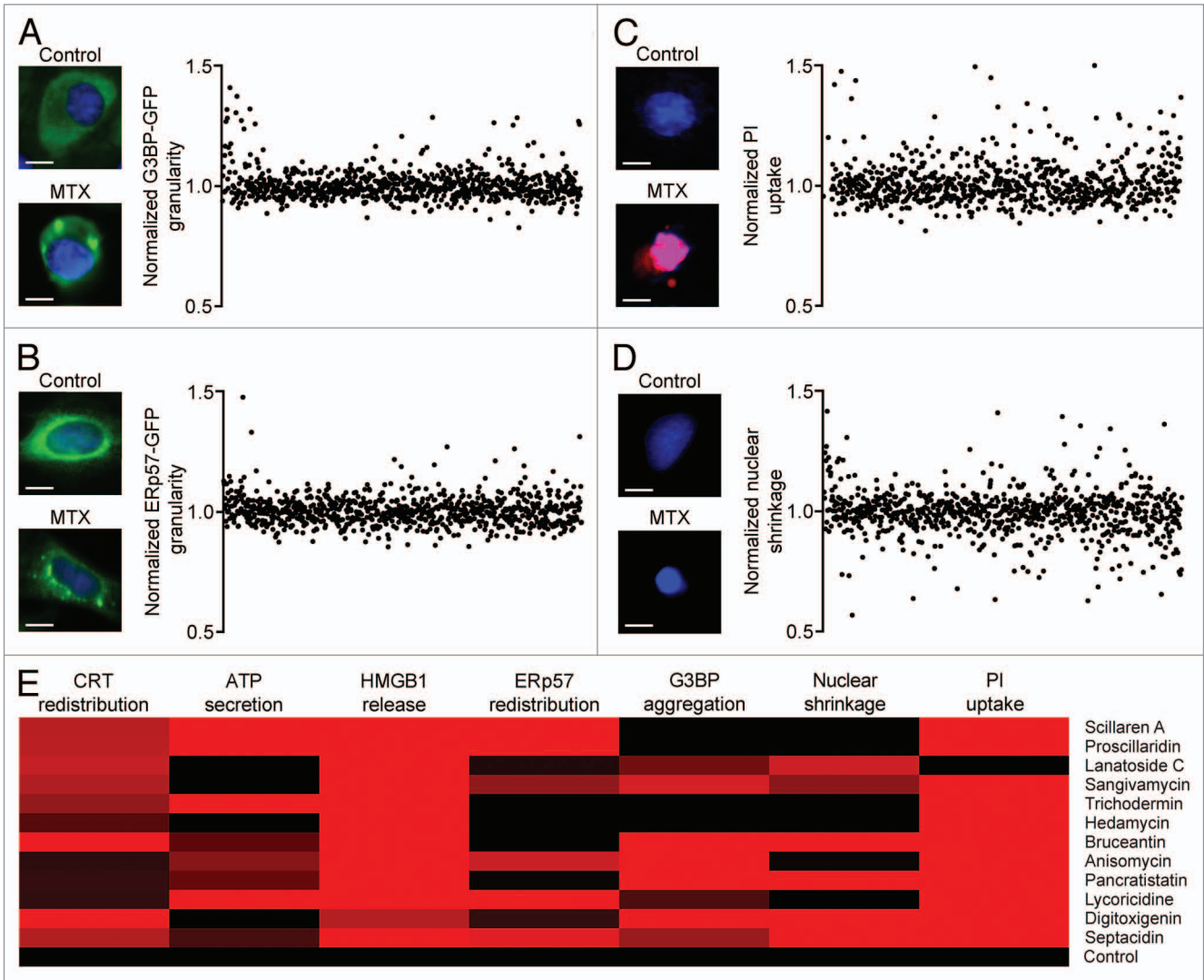


Figure 2. Identification of stress responses accompanying immunogenic cell death. (A–D) Human osteosarcoma U2OS cells stably expressing G3BP-GFP or ERp57-GFP were treated with compounds from the NCI Mechanistic Diversity Set (final concentration = 1 μM) for 4 or 12 h, followed by the assessment of G3BP-GFP aggregation (A) ERp57-GFP redistribution (B) propidium iodide (PI) uptake (C) or nuclear shrinkage (D) by automated fluorescence microscopy. Representative images (scale bars = 10 μm) and quantitative data—ranked as per cumulative immunogenic cell death (ICD) score (see Fig. 1D)—are reported. Each point represents the average of duplicate assessments obtained for each drug, upon intra-plate normalization. (E) The normalized scores for CRT-GRP redistribution, loss of quinacrine-dependent fluorescence, HMGB1 release, ERp57-GFP redistribution, G3BP-GFP aggregation, PI uptake and nuclear shrinkage of the putative ICD inducers identified within the NCI Mechanistic Diversity Set as depicted in Figure 1 are reported in the form of heat map.

to an underlying cardiac condition) exhibited an improved disease outcome as compared with control patients (matched on several clinicopathological parameters) who received chemotherapy alone. Notably, this clinical benefit could not be documented among patients treated with ICD inducers, reinforcing the notion that cardiac glycosides exert antineoplastic effects mostly as they stimulate the immunogenicity of cell death.³⁴⁻³⁶ These findings demonstrate that the detection of ICD surrogate markers in vitro has the potential to drive the discovery of novel ICD inducers.

Based on these premises, we decided to screen the NCI Mechanistic Diversity Set for novel ICD inducers by means of our automated platform. We report here the results of this

screen, allowing us to add septacidin, an antifungal antibiotic produced by *Streptomyces fibriatus*, to the growing list of bona fide ICD inducers.

Results

Screening of the NCI Mechanistic Diversity Set for candidate ICD inducers

Based on an automated screening platform previously developed by us,³⁴ we determined the 3 main hallmarks of ICD in human osteosarcoma U2OS cells exposed to each of the 879 chemicals included in the NCI Mechanistic Diversity Set (final

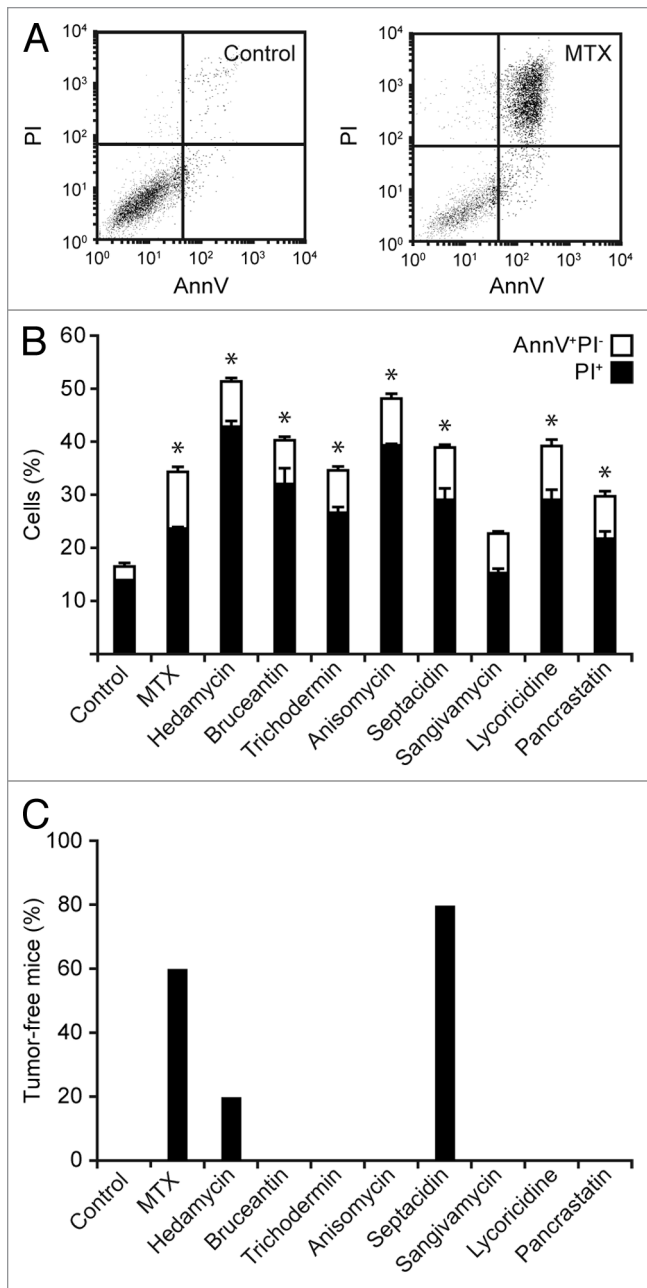


Figure 3. Immunogenic cell death-inducing potential of selected compounds from the NCI Mechanistic Diversity Set. **(A and B)** Mouse fibrosarcoma MCA205 cells were left untreated or treated with 2 μ M mitoxantrone (MTX) or 10 μ M hedamycin, bruceantin, trichodermin, anisomycin, septacidin, sangivamycin, lycoricidine, or pancrastatin for 24 h, followed by the cytofluorometric assessment of phosphatidylserine exposure and plasma membrane permeabilization upon co-staining with FITC-AnnexinV and propidium iodide (PI). Representative dot plots are reported in **A**. In **B**, white and black columns illustrated the percentage of dying (PI⁻AnnV⁺) and dead (PI⁺) cells, respectively (means \pm SEM, $n = 3$). * $P < 0.05$ (unpaired, 2-tailed Student's t test), as compared with untreated cells. **(C)** MCA205 cells were treated as in **A and B**, counted, and used to vaccinate immunocompetent C57BL/6 mice ($n = 5$ per group) that were re-challenged 7 d later with living cells of the same type. Control animals ($n = 5$) were vaccinated with an equivalent volume of PBS. Columns indicate the percentage of mice that were tumor-free 1 mo after re-challenge.

concentration = 1 μ M). In particular, we monitored and quantified the redistribution of a green fluorescence protein (GFP)-tagged variant of CRT from a diffuse to a granular pattern (4 h post-treatment, **Figure 1A**), the loss of ATP-dependent intracellular quinacrine fluorescence (24 h posts-treatment, **Figure 1B**), and the initial steps of the release of a HMGB1-GFP chimera, i.e., its relocalization to the cytoplasm (48 h post-treatment, **Figure 1C**). By summing up the normalized scores individually associated with these phenomena we computed a cumulative ICD score to identify potential ICD inducers (**Fig. 1D and Table S1**). In line with previous results,³⁴ the top 1 percentile of the corresponding rank included several cardiac glycosides (namely, scillaren A, proscillaridin, lanatoside, and digitoxigenin).

Links between stress pathways elicited by the NCI Mechanistic Diversity Set

ICD originates from the activation of a stereotyped ensemble of stress- and death-related signal transduction cascades, among which the ER stress response plays a prominent role.^{14,22,23} We therefore measured 2 distinct ER-stress related and 2 distinct cell death-related phenomena in U2OS cells exposed to each of the 879 compounds contained in the NCI Mechanistic Diversity Set. In particular, we monitored the ER stress response by quantifying the accumulation of stalled translation foci by means of a GFP-tagged variant of GTPase activating protein (SH3 domain) binding protein 1 (GTBP1, best known G3BP) (**Fig. 2A**),³⁷ or the redistribution of the CRT-interacting partner protein disulfide isomerase family A, member 3 (PDIA3, best known as ERp57) fused to GFP from a diffuse to a granular pattern (**Fig. 2B**).³⁸ Moreover, we followed the incorporation of a vital dye (propidium iodide, PI) by cells that underwent plasma membrane permeabilization, a marker of primary as well as post-apoptotic necrosis (**Fig. 2C**),^{39,40} and the reduction of nuclear size that is associated with primary apoptosis, which can be detected upon staining with the cell-permeant chromatinophylic dye Hoechst 33342 (**Fig. 2D**).^{41,42} We observed that the ability of the putative ICD inducers identified within the NCI Mechanistic Diversity Set (**Fig. 1D**) to promote the redistribution of CRT-GFP and ERp57 was not always comparable. Thus, while some of these agents (e.g., scillaren A) appear to operate like anthracyclines, promoting the co-exposure of CRT and ERp57 on the cell surface,³⁸ others (e.g., lanatoside C) resemble hypericin-based photodynamic therapy, which cause ICD independently of the translocation of ERp57 on the outer leaflet of the plasma membrane (**Fig. 2E**).^{19,20} Along similar lines, we failed to observe a stringent parallelism between the formation of stress granules and the redistribution of CRT or ERp57 (**Fig. 2E**), suggesting that the signaling cascades elicited by these putative ICD inducers involve multiple manifestations of the ER stress response that cannot easily be linked to each other. Finally, we found that all the potentially immunogenic agents identified within the NCI Mechanistic Diversity Set induce either chromatin condensation in the absence of plasma membrane permeabilization (reflecting the first steps of apoptosis), either plasma membrane permeabilization in the absence of chromatin condensation (reflecting primary necrosis), or both (reflecting post-apoptotic necrosis) (**Fig. 2E**). These findings indicate that besides promoting the secretion of ATP

and the release of HMGB1, the molecules identified in our screen also trigger 1 or more manifestations of ER stress and exert a cytotoxic activity against human osteosarcoma U2OS cells.

Validation of hits on murine cancer cells

To determine the actual immunogenic potential of the putative ICD inducers that we identified within the NCI Mechanistic Diversity Set (Fig. 1D), we first tested the cytotoxic potential of these agents (excluding cardiac glycosides) on MCA205 cells, methylcholanthrene-induced fibrosarcoma cells derived from a female C57BL/6 mouse.⁴³ Thus, the exposure of MCA205 cells to 10 μ M hedamycin, bruceantin, trichodermin, anisomycin, septacidin, lycoricidine, or pancrastatin for 24 h resulted in the accumulation of cells exposing phosphatidylserine on the outer leaflet of the plasma membrane (an early sign of apoptosis) or taking up the vital dye PI (an indication of plasma membrane permeabilization), as determined by conventional cytofluorometric assays (Fig. 3A and B). This was not the case of sangivamycin, which was unable to induce signs of incipient apoptosis in cultured MCA205 cells upon a 24 h incubation (Fig. 3B).

Thereafter, we set out to test the capacity of all these chemicals to induce bona fide ICD by the gold-standard approach, i.e., vaccination experiments in histocompatible mice.¹⁴ To this aim, MCA205 cells were treated with 10 μ M hedamycin, bruceantin, trichodermin, anisomycin, septacidin, sangivamycin, lycoricidine, or pancrastatin for 24 h, washed, and injected (5×10^5 cells) s.c. into the right flank of C57BL/6 mice (5 per group). One week later, these animals were re-challenged with 1×10^5 cells living MCA205 cells, which were injected s.c. into the contralateral (left) flank. Mice were then routinely examined for tumor growth, and the absence of palpable neoplastic lesions was interpreted as a sign of protective anticancer immunity. Of note, MCA205 cells succumbing to only 2 candidate ICD inducers were able to protect at least 1 mouse against the establishment of homologous tumors: hedamycin (1/5 mice) and septacidin (4/5 mice) (Fig. 3C). Mitoxantrone-treated MCA205 cells, which were employed as a positive control, protected 3/5 animals from a re-challenge with malignant cells of the same type (Fig. 3C). Of note, MCA205 cells dying in response to sangivamycin failed to confer protective immunity to C57BL/6 mice, yet allowed them to control tumor growth, as all re-challenged animals (5/5) had significantly smaller tumors than their control counterparts (data not shown). Next, we tested MCA205 cells exposed to hedamycin, septacidin, and sangivamycin for (1) CRT surface exposure, by immunofluorescence in conjunction with cytofluorometry (Fig. 4A and B), (2) loss of intracellular ATP, by quinacrine staining and cytofluorometry (Fig. 4C and D), (3) accumulation of

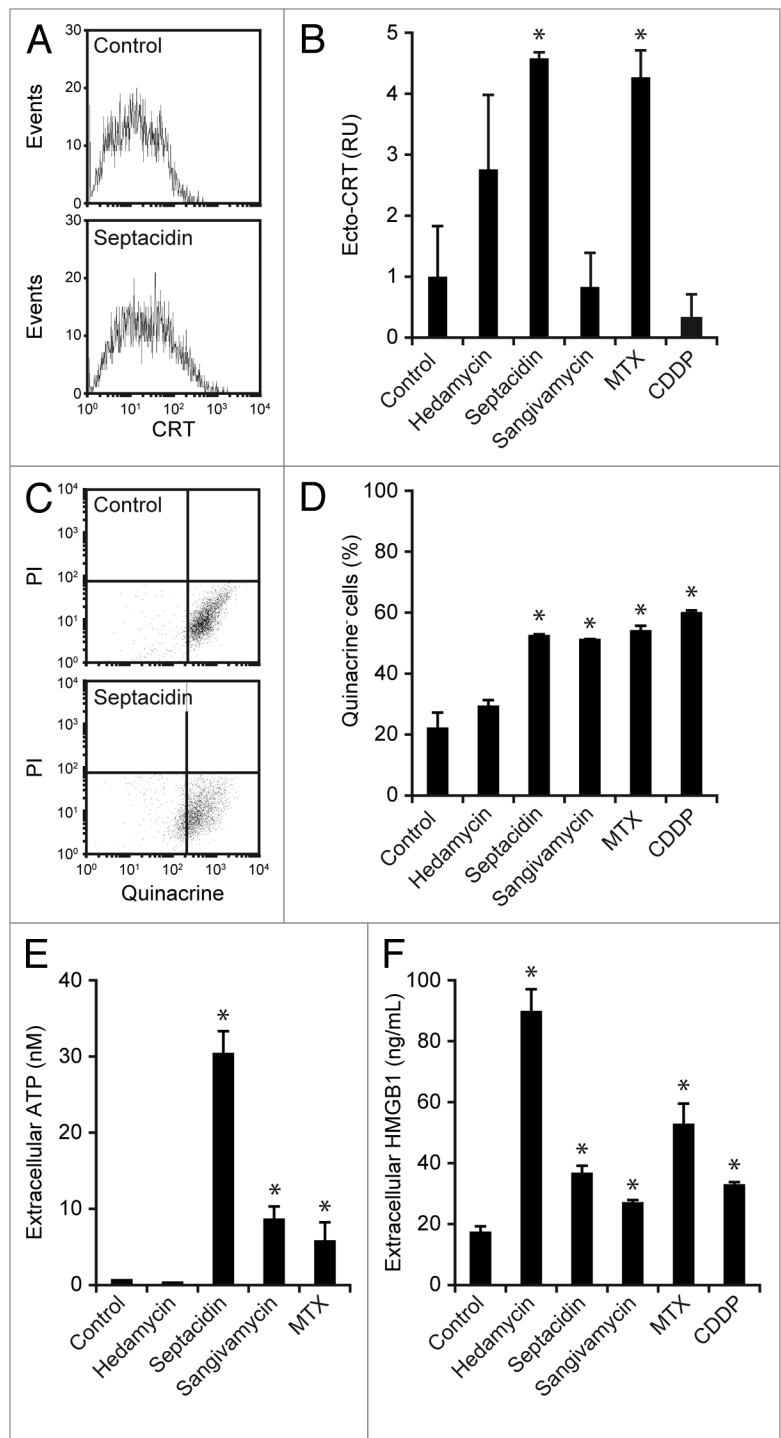


Figure 4. Ability of selected compounds from the NCI Mechanistic Diversity Set to elicit immunogenic cell death hallmarks in murine cells. (A–F) Mouse fibrosarcoma MCA205 cells were left untreated or treated with 2 μ M mitoxantrone (MTX), 300 μ M cisplatin (CDDP) or 10 μ M hedamycin, septacidin, or sangivamycin for 24 h followed by the assessment of calreticulin (CRT) exposure on living cells by indirect immunofluorescence in conjunction with cytofluorometry (A and B), loss of quinacrine-dependent fluorescence by cytofluorometry (C and D), extracellular ATP levels by a luciferase-based assay (E) and extracellular HMGB1 concentrations by ELISA (F). Representative dot plots are illustrated in A and C, while quantitative data means \pm SEM, n = 3) are reported in B, D, E, and F. * P < 0.05 (unpaired, 2-tailed Student's t test), as compared with untreated cells.

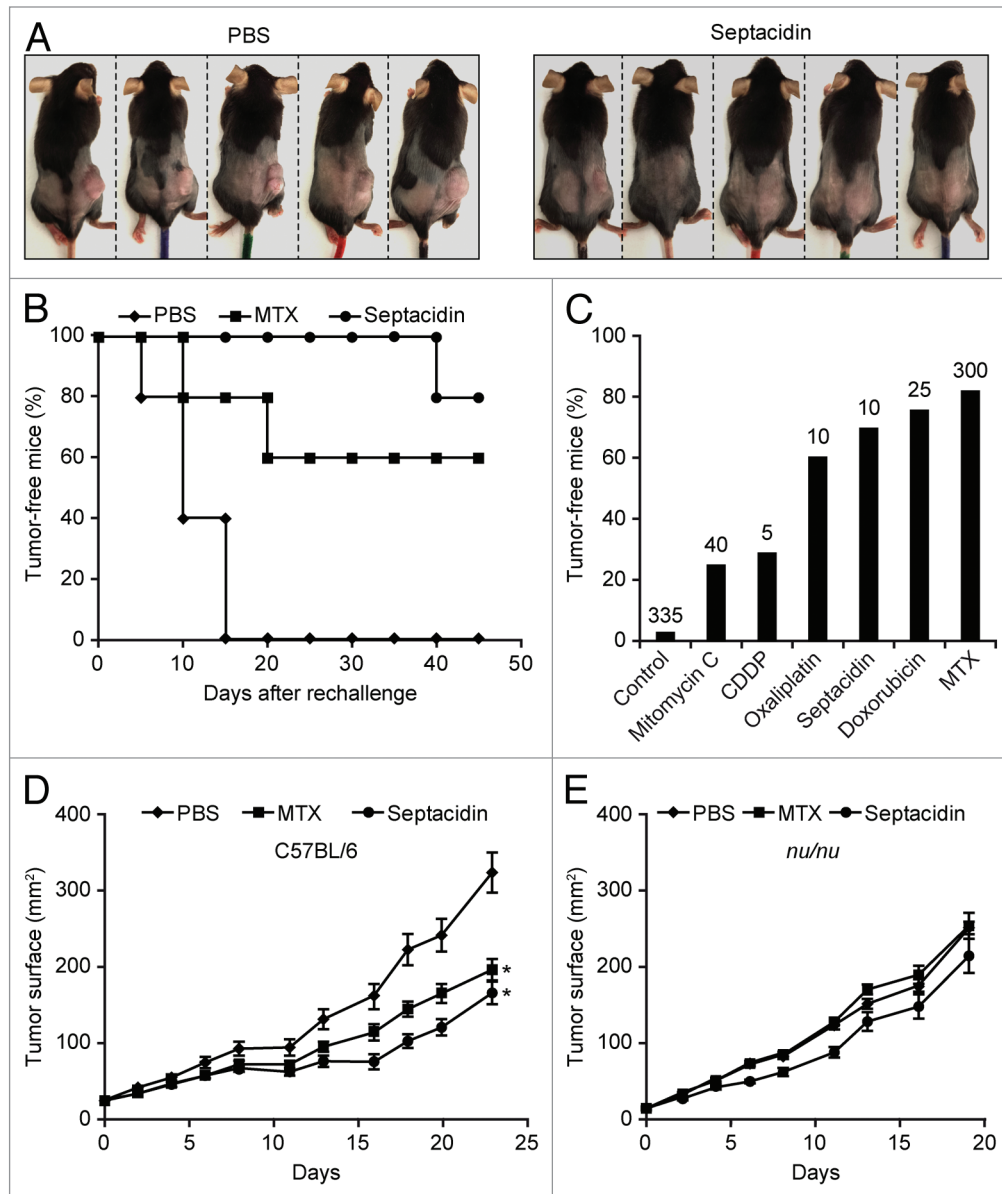


Figure 5. Capacity of septacidin to induce bona fide immunogenic cell death. **(A and B)** Murine fibrosarcoma MCA205 cells were treated with 10 μ M septacidin for 24 h and used to vaccinate C57BL/6 mice ($n = 5$), which were re-challenged 1 wk later with living cells of the same type. Control animals ($n = 5$) were vaccinated with an equivalent volume of PBS. Tumor incidence was routinely monitored thereafter. Representative images taken on day 45 are depicted in **A**. Panel **B** reports the evolution of tumor incidence over time as a Kaplan–Meier curve. **(C)** Comparison of the ability of septacidin to promote the immunogenic demise of mouse fibrosarcoma MCA205 cells with that of other immunogenic cell death (ICD) inducers, as per published and unpublished vaccination experiments. Columns report the percentage of mice that failed to develop tumors upon vaccination with MCA205 cells succumbing to the indicated molecule and re-challenge (1 wk later) with living tumor cells of the same type. The number of animals globally employed for these determinations is indicated. **(D and E)** Living MCA205 cells were injected s.c. into wild-type **(D)** or *nu/nu* C57BL/6 mice **(E)** and tumor growth was routinely monitored thereafter. When tumor surface reached 30–40 mm², mice ($n = 5$ per group) received 7.78 mg/kg septacidin, 0.33 mg/kg mitoxantrone (MTX) or an equivalent volume of PBS, as a single intratumoral injection. * = $P < 0.05$ (Log-rank test), as compared with PBS-treated animals.

extracellular ATP, by means of a luciferase-based assay (Fig. 4E), and (4) HMGB1 release, with a commercially available ELISA (Fig. 4F). Mitoxantrone and cisplatin, an oxaliplatin-like agent that is unable to trigger ICD,^{37,44,45} were employed as positive and negative controls, respectively. Although hedamycin induced a robust release of HGBM1 by MCA205 cells (Fig. 4F), consistent with its robust cytotoxicity (Fig. 3B), it failed to promote CRT exposure and ATP secretion (Fig. 4B, D, and E).

Sangivamycin-treated MCA205 cells secreted ATP and released HMGB1 (Fig. 4D–F), yet did not expose CRT on their surface (Fig. 4B). Septacidin was the only of these agents to consistently induce all the hallmarks of ICD in MCA205 cells, in thus far resembling mitoxantrone (Fig. 4B and D–F)

Driven by these findings, we decided to validate the ICD-inducing potential of septacidin in a further round of experiments in vivo. In this setting, septacidin-killed MCA205 cells protected

4/5 (80%) C57BL/6 mice against a re-challenge with living cells of the same type (Fig. 5A and B). A comprehensive analysis of relevant scientific literature demonstrated that this is in line with the protective potential of cell death triggered by established ICD inducers (Fig. 5C), including oxaliplatin (80% protection),⁴⁴ doxorubicin (90% protection),⁴⁶ and mitoxantrone (80% protection).²² In addition, the intratumoral injection of septacidin significantly reduced the growth of MCA205 fibrosarcomas evolving in immunocompetent mice (Fig. 5D), but not in their *nu/nu* counterparts (Fig. 5E), which lack T lymphocytes. This latter result confirms the capacity of septacidin to mediate anticancer effects that at least in part depend on the immune system.

Discussion

In this study, we validated the capacity of an automated screening platform that we developed to identify ICD inducers within large chemical libraries. In 2012, we first employed this platform to screen all FDA-approved anticancer agents, leading to the discovery that cardiac glycosides can convert non-immunogenic instances of cell death into bona fide ICD.³⁴ In the present study, we adopted a similar strategy to screen the NCI Mechanistic Diversity Set for potential ICD inducers. In a first round of experiments, the compounds included in this library were monitored for their ability to induce the redistribution of a CRT-GFP chimera (4 h post-exposure), the loss of quinacrine-dependent fluorescence (24 h post-exposure), and the release of a HMGB1-GFP fusion protein (48 h post-exposure) in human osteosarcoma U2OS cells. Next, the activity of candidate ICD inducers was validated in vitro, in low-throughput assays based on murine fibrosarcoma MCA205 cells, as well as in vivo, in gold-standard vaccination and chemotherapy experiments involving MCA205 cells and syngeneic C57BL/6 mice. This approach led to the discovery of at least 1 novel ICD inducer, septacidin, confirming that this platform is suitable for the identification of chemicals that promote the immunogenic demise of malignant cells within large libraries.

Although the overall design of our screening approach appears to be suitable for the identification of novel ICD inducers, there are a few potential limitations that should be taken into consideration. First, the compounds of the NCI Mechanistic Diversity Set were tested at a homogenous concentration chosen arbitrarily (1 μ M) and at a limited number of time points. This implies that hypothetical agents capable of stimulating surrogate ICD markers at a different concentration or with a different kinetics went undetected. To limit the number of such false-negative results, it may be necessary to perform multiple rounds of screening involving large dose ranges and/or kinetic evaluations. Second, our screening relied on a single type of malignant cells, namely, U2OS osteosarcoma cells. As human cancer cells respond to antineoplastic agents with a high degree of heterogeneity,⁴⁷ it might be advisable to express the fluorescent biosensors used in this study (i.e., the CRT-GFP and HMGB1-GFP chimeras) in distinct cancer cell lines and use them in parallel screening efforts. Third, although the initial screening was performed on

human cancer cells, validation was performed in the murine system (MCA205 fibrosarcoma cells and histocompatible C57BL/6 mice). Thus, species-specific differences in the efficacy of the chemicals identified by the primary screen may yield false-negative results at validation. Although we attempted to minimize this possibility (by increasing the drug concentration used in validation experiments to 10 μ M), it might be advisable to take advantage of so-called “humanized” mouse models, allowing for the inoculation of human cancer cells into mice that bear a human immune system (and hence do not reject the graft based on species incompatibility).⁴⁸ Thus, our screening approach is admittedly perfectible.

Notwithstanding these caveats, the number of ICD inducers identified within the NCI Mechanistic Diversity Set was surprisingly low. Indeed, only 1 out of 879 agents (~100 of which killed U2OS cells in vitro) could be characterized as a bona fide ICD inducer acting across species barriers. Unfortunately, no in-depth information is available on the mode of action of this agent, septacidin, an antifungal antibiotic produced by *Streptomyces fibriatus*.⁴⁹ However, it is tempting to speculate that this microbial product may provoke an ultimately lethal stress response in mammalian cells upon the activation of pattern recognition receptors.⁵⁰ This possibility will be actively investigated in our laboratory.

The fact that the percentages of bona fide ICD inducers identified within the NCI Mechanistic Diversity Set (< 1%) and among FDA-approved antineoplastic agents (> 5%) are significantly different from each other may reflect the rather distinct history of these drug collections. The Mechanistic Diversity Set was indeed constructed starting from preclinical data on growth inhibition, as obtained on 60 distinct human cancer cell lines (source http://dtp.nci.nih.gov/branches/dscb/mechanistic_explanation.html). Conversely, the efficacy of all FDA-approved anticancer agents has been documented in clinical trials, a process that may have empirically favored the selection of ICD inducers.^{3,4}

In essence, the present report describes a general strategy for the identification of ICD inducers within large chemical libraries. By this approach, we demonstrated that septacidin, an antifungal antibiotic produced by *Streptomyces fibriatus*, mediates antitumor effects that for the most part (if not entirely) depended on the elicitation of an anticancer immune response.

Materials and Methods

Chemicals, cell lines, and culture conditions

Unless otherwise specified, chemicals were obtained from Sigma–Aldrich, media and supplements for cell cultures from Life Technologies Inc., and plasticware from Corning Inc. Murine fibrosarcoma MCA205 cells (Class I MHC haplotype H-2^b, histocompatible with C57BL/6 mice) and human osteosarcoma U2OS cells were cultured in RPMI-1640 medium and Dulbecco’s modified Eagle’s medium (DMEM), respectively. In both cases, cells were maintained in standard culture conditions (37 °C and 5% CO₂) and media were supplemented with 10% (v/v) fetal

bovine serum (FBS), 1 mM sodium pyruvate, 10 mM HEPES, 10 U/mL penicillin sodium, and 10 µg/mL streptomycin sulfate. U2OS cells stably co-expressing a histone 2B-red fluorescent protein fusion (H2B-RFP) and GFP fused to either CRT (CRT-GFP) or HMGB1 (HMGB1-GFP) were maintained in the continuous presence of 200 µg/mL zeocine plus 1 µg/mL blasticidine and 200 µg/mL G418 plus 1 µg/mL blasticidine, respectively. U2OS cells stably expressing either G3PB or ERp57 fused to GFP (G3BP-GFP or ERp57-GFP) were cultured in the continuous presence of 200 µg/mL zeocine or 200 µg/mL G418, respectively.

High-throughput screen for CRT-/ERp57-exposing and HMGB1-/ATP-releasing drugs

5 × 10³ U2OS cells stably co-expressing H2B-RFP and CRT-GFP or Erp57-GFP or HMGB1-GFP or G3BP-GFP were seeded into 96-well poly-*L*-lysine-pretreated Black/Clear imaging plates (BD Biosciences) and allowed to adapt for 24 h. Thereafter, each compound of the NCI Mechanistic Diversity Set was added at a final concentration of 1 µM, and cells were incubated for additional 4, 24, or 48 h before fixation in PBS supplemented with 1 µg/mL Hoechst 33342 and 4% (w/v) paraformaldehyde for 20 min. Upon fixation, PFA was substituted with PBS and 4 view fields per well were acquired by means of a BD Pathway 855 Automated Bioimager (BD Biosciences), equipped with a UApo/340 × 20/0.75 objective (Olympus). Subsequently, images were segmented and analyzed for GFP granularity or HMGB1-GFP nuclear intensity using the BD AttoVision software v. 1.7 (BD Biosciences). To monitor ATP secretion, wild-type U2OS cells treated with the compounds of the NCI Mechanistic Diversity Set for 24 h were labeled with quinacrine as previously described.³⁷ Briefly, cells were stained with Krebs-Ringer solution (125 mM NaCl, 5 mM KCl, 1 mM MgSO₄, 0.7 mM KH₂PO₄, 2 mM CaCl₂, 6 mM glucose, and 25 mM HEPES, pH 7.4) supplemented with 1 µM quinacrine (Life Technologies Inc.) for 30 min at 37 °C. Thereafter, cells were incubated with 1 µg/mL PI and 1 µg/mL Hoechst 33342 (both from Life Technologies Inc.) for 10 min and rinsed with Krebs-Ringer solution. Finally, cells were examined on a BD Pathway 855 Automated Bioimager equipped with a UApo/340 × 20/0.75 objective. Nuclear morphology was monitored in parallel to all determinations described above as an indicator of cell death. Data were mined and statistically evaluated using the Prism software v. Five (Graph Pad software Inc.). Intra-plate normalization was obtained by calculating the ratio of each experimental value to the mean of all values associated with the same compound within the same plate.

Determination of cell surface-exposed CRT by immunofluorescence

Cells were harvested and washed with ice-cold PBS, then incubated with a CRT-specific antibody (Abcam) diluted in cold blocking buffer (5% FBS, v/v in PBS) for 30 min on ice, washed, and incubated with an AlexaFluor® 488-conjugated antibody (Life Technologies Inc.) in blocking buffer (for 30 min). Thereafter, cells were washed, stained with 1 µg/mL PI in cold PBS for 5 min, and analyzed by means of a FACSCalibur cytofluorometer (BD Biosciences). Isotype-matched IgG

antibodies (Cell Signaling Technology) were used as negative staining control. First line statistical analyses were performed by using the CellQuest™ software (BD Biosciences), upon gating on PI⁺ events characterized by normal forward and side scatter (living cells).

Determination of extracellular HMGB1 and ATP concentrations

Extracellular HMGB1 was quantified by means of the HMGB1 ELISA Kit II (Shino Test Corp.), following the manufacturer's instructions. Extracellular ATP concentrations were determined by the luciferase/luciferin-based ENLITEN ATP Assay (Promega), as recommended by the manufacturer. Absorbance and chemiluminescence were measured on a Fluostar OPTIMA multi-label reader (BMG Labtech).

Quantification of cell death

Cell death was assessed by means of the FITC-AnnexinV Detection Kit I (BD Biosciences), as per standardized procedures.⁵¹ Briefly, 10⁵ cells were collected per sample, washed in PBS, and resuspended in 1X binding buffer (10 mM HEPES/NaOH - pH 7.4, 140 mM NaCl, and 5 mM CaCl₂) containing fluorescein isothiocyanate (FITC)-conjugated AnnexinV (BD Biosciences) and 0.5 µg/mL PI, following the manufacturer's instructions. Cytofluorometric determinations were performed on a FACSCalibur cytofluorometer equipped with a 70 µm nozzle. First line statistical analyses were performed by using the CellQuest™ software (BD Biosciences), by gating on the events characterized by normal forward and side scatter.

Vaccination and chemotherapy experiments

All animal experiments were approved by the local Ethics Committee (CEEA IRCIV / IGR n°26, registered with the French Ministry of Research), and complied with the 63/2010/EU directive from the European Parliament. Wild-type and nude (*nu/nu*) C57BL/6 mice (Harlan) were housed in a temperature-controlled environment with 12 h light/dark cycles and received food and water ad libitum. Murine fibrosarcoma MCA205 cells were incubated with either 2 µM mitoxantrone or 10 µM hedamycin, bruceantin, trichodermin, anisomycin, septacidin, sangivamycin, lycoricidine, or pancrastatin for 24 h, and inoculated (5 × 10⁵ cells) s.c. into the left flanks of 6-wk old female C57BL/6 mice. Seven days later, mice received 1 × 10⁵ living MCA205 cells s.c. in the right flank. Tumor incidence was monitored routinely thereafter, and the absence of tumors was scored as an indication for antitumor vaccination. For chemotherapy experiments, 2 × 10⁵ MCA205 cells were inoculated s.c. into the left flank of wild-type and *nu/nu* C57BL/6 mice and tumor growth was routinely monitored thereafter by means of a standard caliper. When tumor surface reached 30–40 mm², mice (n = 5 per group) were randomly assigned to receive either 7.78 mg/kg septacidin (as a single intratumoral injection in PBS) either 0.33 mg/kg mitoxantrone (as a single intraperitoneal injection in PBS), or an equivalent volume of PBS (negative control condition)

Statistical analyses

Statistical analyses were performed with the Microsoft Office software package (Microsoft). Tumor growth curves were compared with the Log-rank test. Pairwise data comparisons

were performed by means of the unpaired, 2-tailed Student's *t* test. All *P* values < 0.05 were considered statistically significant.

Disclosure of Potential Conflicts of Interest

No potential conflicts of interest were disclosed.

Acknowledgments

We thank the National Cancer Institute (NCI) for the generous supply of drug libraries. This work is supported by the Ligue contre le Cancer (équipe labellisée); Agence National de la Recherche

(ANR); Association pour la recherche sur le cancer (ARC); Cancéropôle Ile-de-France; Institut National du Cancer (INCa); Fondation Bettencourt-Schueller; Fondation de France; Fondation pour la Recherche Médicale (FRM); the European Commission (ArtForce); the European Research Council (ERC); the LabEx Immuno-Oncology; the SIRIC Stratified Oncology Cell DNA Repair and Tumor Immune Elimination (SOCRATE); the SIRIC Cancer Research and Personalized Medicine (CARPEM); and the Paris Alliance of Cancer Research Institutes (PACRI).

References

- Zitvogel L, Tesniere A, Kroemer G. Cancer despite immunosurveillance: immunoselection and immunosubversion. *Nat Rev Immunol* 2006; 6:715-27; PMID:16977338; <http://dx.doi.org/10.1038/nri1936>
- Zitvogel L, Apetoh L, Ghiringhelli F, Kroemer G. Immunological aspects of cancer chemotherapy. *Nat Rev Immunol* 2008; 8:59-73; PMID:18097448; <http://dx.doi.org/10.1038/nri2216>
- Zitvogel L, Galluzzi L, Smyth MJ, Kroemer G. Mechanism of action of conventional and targeted anticancer therapies: reinstating immunosurveillance. *Immunity* 2013; 39:74-88; PMID:23890065; <http://dx.doi.org/10.1016/j.immuni.2013.06.014>
- Galluzzi L, Senovilla L, Zitvogel L, Kroemer G. The secret aly: immunostimulation by anticancer drugs. *Nat Rev Drug Discov* 2012; 11:215-33; PMID:22301798; <http://dx.doi.org/10.1038/nrd3626>
- Hervieu A, Mignot G, Ghiringhelli F. Dacarbazine mediate antimelanoma effects via NK cells. *Oncoimmunology* 2013; 2:e23714; PMID:23734324; <http://dx.doi.org/10.4161/onci.23714>
- Ghiringhelli F, Bruchard M, Apetoh L. Immune effects of 5-fluorouracil: Ambivalence matters. *Oncoimmunology* 2013; 2:e23139; PMID:23802066; <http://dx.doi.org/10.4161/onci.23139>
- Mignot G, Bugaut H, Ghiringhelli F. Immune ambivalence: The schizophrenic bleomycin. *Oncoimmunology* 2013; 2:e25737; PMID:24327935; <http://dx.doi.org/10.4161/onci.25737>
- Mattarollo SR, West AC, Steegh K, Duret H, Paget C, Martin B, Matthews GM, Shortt J, Chesi M, Bergsagel PL, et al. NKT cell adjuvant-based tumor vaccine for treatment of myc oncogene-driven mouse B-cell lymphoma. *Blood* 2012; 120:3019-29; PMID:22932803; <http://dx.doi.org/10.1182/blood-2012-04-426643>
- Ma Y, Adjemian S, Mattarollo SR, Yamazaki T, Aymeric L, Yang H, Portela Catani JP, Hannani D, Duret H, Steegh K, et al. Anticancer chemotherapy-induced intratumoral recruitment and differentiation of antigen-presenting cells. *Immunity* 2013; 38:729-41; PMID:23562161; <http://dx.doi.org/10.1016/j.immuni.2013.03.003>
- Ma Y, Mattarollo SR, Adjemian S, Yang H, Aymeric L, Hannani D, Portela Catani JP, Duret H, Teng MW, Kepp O, et al. CCL2/CCR2-dependent recruitment of functional antigen-presenting cells into tumors upon chemotherapy. *Cancer Res* 2014; 74:436-45; PMID:24302580; <http://dx.doi.org/10.1158/0008-5472.CAN-13-1265>
- Ma Y, Yamazaki T, Yang H, Kepp O, Galluzzi L, Zitvogel L, Smyth MJ, Kroemer G. Tumor necrosis factor is dispensable for the success of immunogenic anticancer chemotherapy. *Oncoimmunology* 2013; 2:e24786; PMID:23894723; <http://dx.doi.org/10.4161/onci.24786>
- Michaud M, Sukkurwala AQ, Martins I, Shen S, Zitvogel L, Kroemer G. Subversion of the chemotherapy-induced anticancer immune response by the ecto-ATPase CD39. *Oncoimmunology* 2012; 1:393-5; PMID:22737627; <http://dx.doi.org/10.4161/onci.19070>
- Hannsdóttir L, Tymozzuk P, Parajuli N, Wasmer MH, Philipp S, Daschil N, Datta S, Koller JB, Tripp CH, Stoitzner P, et al. Lapatinib and doxorubicin enhance the Stat1-dependent antitumor immune response. *Eur J Immunol* 2013; 43:2718-29; PMID:23843024; <http://dx.doi.org/10.1002/eji.201242505>
- Kroemer G, Galluzzi L, Kepp O, Zitvogel L. Immunogenic cell death in cancer therapy. *Annu Rev Immunol* 2013; 31:51-72; PMID:23157435; <http://dx.doi.org/10.1146/annurev-immunol-032712-100008>
- Garg AD, Martin S, Golab J, Agostinis P. Danger signalling during cancer cell death: origins, plasticity and regulation. *Cell Death Differ* 2014; 21:26-38; PMID:23686135; <http://dx.doi.org/10.1038/cdd.2013.48>
- Krysko DV, Garg AD, Kaczmarek A, Krysko O, Agostinis P, Vandenabeele P. Immunogenic cell death and DAMPs in cancer therapy. *Nat Rev Cancer* 2012; 12:860-75; PMID:23151605; <http://dx.doi.org/10.1038/nrc3380>
- Vacchelli E, Galluzzi L, Fridman WH, Galon J, Sautès-Fridman C, Tartour E, Kroemer G. Trial watch: Chemotherapy with immunogenic cell death inducers. *Oncoimmunology* 2012; 1:179-88; PMID:22720239; <http://dx.doi.org/10.4161/onci.1.2.19026>
- Vacchelli E, Senovilla L, Eggermont A, Fridman WH, Galon J, Zitvogel L, Kroemer G, Galluzzi L. Trial watch: Chemotherapy with immunogenic cell death inducers. *Oncoimmunology* 2013; 2:e23510; PMID:23687621; <http://dx.doi.org/10.4161/onci.23510>
- Garg AD, Krysko DV, Verfaillie T, Kaczmarek A, Ferreira GB, Marysaet L, Rubio N, Firczuk M, Mathieu C, Roebroek AJ, et al. A novel pathway combining calreticulin exposure and ATP secretion in immunogenic cancer cell death. *EMBO J* 2012; 31:1062-79; PMID:22252128; <http://dx.doi.org/10.1038/emboj.2011.497>
- Galluzzi L, Kepp O, Kroemer G. Enlightening the impact of immunogenic cell death in photodynamic cancer therapy. *EMBO J* 2012; 31:1055-7; PMID:22252132; <http://dx.doi.org/10.1038/emboj.2012.2>
- Fucikova J, Kralikova P, Fialova A, Brtnicky T, Rob L, Bartunkova J, Spisek R. Human tumor cells killed by anthracyclines induce a tumor-specific immune response. *Cancer Res* 2011; 71:4821-33; PMID:21602432; <http://dx.doi.org/10.1158/0008-5472.CAN-11-0950>
- Obeid M, Tesniere A, Ghiringhelli F, Fimia GM, Apetoh L, Perfettini JL, Castedo M, Mignot G, Panaretakis T, Casares N, et al. Calreticulin exposure dictates the immunogenicity of cancer cell death. *Nat Med* 2007; 13:54-61; PMID:17187072; <http://dx.doi.org/10.1038/nm1523>
- Panaretakis T, Kepp O, Brockmeier U, Tesniere A, Bjorklund AC, Chapman DC, Durchschlag M, Joza N, Pierron G, van Ender P, et al. Mechanisms of pre-apoptotic calreticulin exposure in immunogenic cell death. *EMBO J* 2009; 28:578-90; PMID:19165151; <http://dx.doi.org/10.1038/emboj.2009.1>
- Kepp O, Menger L, Vacchelli E, Locher C, Adjemian S, Yamazaki T, Martins I, Sukkurwala AQ, Michaud M, Senovilla L, et al. Crosstalk between ER stress and immunogenic cell death. *Cytokine Growth Factor Rev* 2013; 24:311-8; PMID:23787159; <http://dx.doi.org/10.1016/j.cytogfr.2013.05.001>
- Ghiringhelli F, Apetoh L, Tesniere A, Aymeric L, Ma Y, Ortiz C, Vermaelen K, Panaretakis T, Mignot G, Ullrich E, et al. Activation of the NLRP3 inflammasome in dendritic cells induces IL-1beta-dependent adaptive immunity against tumors. *Nat Med* 2009; 15:1170-8; PMID:19767732; <http://dx.doi.org/10.1038/nm.2028>
- Martins I, Tesniere A, Kepp O, Michaud M, Schlemmer F, Senovilla L, Séror C, Métivier D, Perfettini JL, Zitvogel L, et al. Chemotherapy induces ATP release from tumor cells. *Cell Cycle* 2009; 8:3723-8; PMID:19855167; <http://dx.doi.org/10.4161/cc.8.22.10026>
- Michaud M, Martins I, Sukkurwala AQ, Adjemian S, Ma Y, Pellegatti P, Shen S, Kepp O, Scoazec M, Mignot G, et al. Autophagy-dependent anticancer immune responses induced by chemotherapeutic agents in mice. *Science* 2011; 334:1573-7; PMID:22174255; <http://dx.doi.org/10.1126/science.1208347>
- Martins I, Wang Y, Michaud M, Ma Y, Sukkurwala AQ, Shen S, Kepp O, Métivier D, Galluzzi L, Perfettini JL, et al. Molecular mechanisms of ATP secretion during immunogenic cell death. *Cell Death Differ* 2014; 21:79-91; PMID:23852373; <http://dx.doi.org/10.1038/cdd.2013.75>
- Apetoh L, Ghiringhelli F, Tesniere A, Obeid M, Ortiz C, Criollo A, Mignot G, Maiuri MC, Ullrich E, Saulnier P, et al. Toll-like receptor 4-dependent contribution of the immune system to anticancer chemotherapy and radiotherapy. *Nat Med* 2007; 13:1050-9; PMID:17704786; <http://dx.doi.org/10.1038/nm1622>
- Yamazaki T, Hannani D, Prada N, Adjemian S, Catani JP, Freudenberg M, et al. Defective immunogenic cell death of HMGB1-deficient tumors: compensatory therapy with TLR4 agonists. *Cell Death Differ* 2014; 21:69-78; PMID:23811849; <http://dx.doi.org/10.1038/cdd.2013.72>
- Guerriero JL, Ditsworth D, Zong WX. Non-apoptotic routes to defeat cancer. *Oncoimmunology* 2012; 1:94-6; PMID:22720222; <http://dx.doi.org/10.4161/onci.1.1.17885>
- Kono K, Mimura K. Immunogenic tumor cell death induced by chemoradiotherapy in a clinical setting. *Oncoimmunology* 2013; 2:e22197; PMID:23482346; <http://dx.doi.org/10.4161/onci.22197>

33. Ma Y, Adjemian S, Yang H, Catani JP, Hannani D, Martins I, Michaud M, Kepp O, Sukkurwala AQ, Vacchelli E, et al. ATP-dependent recruitment, survival and differentiation of dendritic cell precursors in the tumor bed after anticancer chemotherapy. *Oncoimmunology* 2013; 2:e24568; PMID:23894718; <http://dx.doi.org/10.4161/onci.24568>
34. Menger L, Vacchelli E, Adjemian S, Martins I, Ma Y, Shen S, Yamazaki T, Sukkurwala AQ, Michaud M, Mignot G, et al. Cardiac glycosides exert anticancer effects by inducing immunogenic cell death. *Sci Transl Med* 2012; 4:143ra99; PMID:22814852; <http://dx.doi.org/10.1126/scitranslmed.3003807>
35. Kepp O, Menger L, Vacchelli E, Adjemian S, Martins I, Ma Y, Sukkurwala AQ, Michaud M, Galluzzi L, Zitvogel L, et al. Anticancer activity of cardiac glycosides: At the frontier between cell-autonomous and immunological effects. *Oncoimmunology* 2012; 1:1640-2; PMID:23264921; <http://dx.doi.org/10.4161/onci.21684>
36. Menger L, Vacchelli E, Kepp O, Eggermont A, Tartour E, Zitvogel L, Kroemer G, Galluzzi L. Trial watch: Cardiac glycosides and cancer therapy. *Oncoimmunology* 2013; 2:e23082; PMID:23525565; <http://dx.doi.org/10.4161/onci.23082>
37. Martins I, Kepp O, Schlemmer F, Adjemian S, Tailler M, Shen S, Michaud M, Menger L, Gdoura A, Tajeddine N, et al. Restoration of the immunogenicity of cisplatin-induced cancer cell death by endoplasmic reticulum stress. *Oncogene* 2011; 30:1147-58; PMID:21151176; <http://dx.doi.org/10.1038/onc.2010.500>
38. Panaretakis T, Joza N, Modjtahedi N, Tesniere A, Vitale I, Durchschlag M, Fimia GM, Kepp O, Piacentini M, Froehlich KU, et al. The co-translocation of ERp57 and calreticulin determines the immunogenicity of cell death. *Cell Death Differ* 2008; 15:1499-509; PMID:18464797; <http://dx.doi.org/10.1038/cdd.2008.67>
39. Kepp O, Galluzzi L, Lipinski M, Yuan J, Kroemer G. Cell death assays for drug discovery. *Nat Rev Drug Discov* 2011; 10:221-37; PMID:21358741; <http://dx.doi.org/10.1038/nrd3373>
40. Vandenabeele P, Galluzzi L, Vanden Berghe T, Kroemer G. Molecular mechanisms of necroptosis: an ordered cellular explosion. *Nat Rev Mol Cell Biol* 2010; 11:700-14; PMID:20823910; <http://dx.doi.org/10.1038/nrm2970>
41. Galluzzi L, Vitale I, Abrams JM, Alnemri ES, Baehrecke EH, Blagosklonny MV, Dawson TM, Dawson VL, El-Deiry WS, Fulda S, et al. Molecular definitions of cell death subroutines: recommendations of the Nomenclature Committee on Cell Death 2012. *Cell Death Differ* 2012; 19:107-20; PMID:21760595; <http://dx.doi.org/10.1038/cdd.2011.96>
42. Galluzzi L, Aaronson SA, Abrams J, Alnemri ES, Andrews DW, Baehrecke EH, Bazan NG, Blagosklonny MV, Blomgren K, Borner C, et al. Guidelines for the use and interpretation of assays for monitoring cell death in higher eukaryotes. *Cell Death Differ* 2009; 16:1093-107; PMID:19373242; <http://dx.doi.org/10.1038/cdd.2009.44>
43. Shu SY, Rosenberg SA. Adoptive immunotherapy of newly induced murine sarcomas. *Cancer Res* 1985; 45:1657-62; PMID:3872168
44. Tesniere A, Schlemmer F, Boige V, Kepp O, Martins I, Ghiringhelli F, Aymeric L, Michaud M, Apetoh L, Barault L, et al. Immunogenic death of colon cancer cells treated with oxaliplatin. *Oncogene* 2010; 29:482-91; PMID:19881547; <http://dx.doi.org/10.1038/onc.2009.356>
45. Galluzzi L, Senovilla L, Vitale I, Michels J, Martins I, Kepp O, Castedo M, Kroemer G. Molecular mechanisms of cisplatin resistance. *Oncogene* 2012; 31:1869-83; PMID:21892204; <http://dx.doi.org/10.1038/onc.2011.384>
46. Casares N, Pequignot MO, Tesniere A, Ghiringhelli F, Roux S, Chaput N, Schmitt E, Hamai A, Hervas-Stubbs S, Obeid M, et al. Caspase-dependent immunogenicity of doxorubicin-induced tumor cell death. *J Exp Med* 2005; 202:1691-701; PMID:16365148; <http://dx.doi.org/10.1084/jem.20050915>
47. Shoemaker RH. The NCI60 human tumour cell line anticancer drug screen. *Nat Rev Cancer* 2006; 6:813-23; PMID:16990858; <http://dx.doi.org/10.1038/nrc1951>
48. Shultz LD, Ishikawa F, Greiner DL. Humanized mice in translational biomedical research. *Nat Rev Immunol* 2007; 7:118-30; PMID:17259968; <http://dx.doi.org/10.1038/nri2017>
49. Dutcher JD, Vonsalta MH, Pansy FE. Septacidin, a New Antitumor and Antifungal Antibiotic Produced by *Streptomyces Fibriatus*. *Antimicrob Agents Chemother (Bethesda)* 1963; 161:83-8; PMID:14275007
50. Vacchelli E, Eggermont A, Sautès-Fridman C, Galon J, Zitvogel L, Kroemer G, Galluzzi L. Trial Watch: Toll-like receptor agonists for cancer therapy. *Oncoimmunology* 2013; 2:e25238; PMID:24083080; <http://dx.doi.org/10.4161/onci.25238>
51. Galluzzi L, Vitale I, Senovilla L, Olaussen KA, Pinna G, Eisenberg T, Goubar A, Martins I, Michels J, Kratassiouk G, et al. Prognostic impact of vitamin B6 metabolism in lung cancer. *Cell Rep* 2012; 2:257-69; PMID:22854025; <http://dx.doi.org/10.1016/j.celrep.2012.06.017>